Synthesis and Structure of $NaGaSn_2$. A Zintl Phase with a Helical Framework Structure

J. T. Vaughey and John D. Corbett*

Contribution from Ames Laboratory and Department of Chemistry, Iowa State University, Ames, Iowa 50011

Received June 11, 1996[⊗]

Abstract: A new Zintl phase $NaGaSn_2$ is obtained pure from stoichiometric reactions of the elements in sealed Ta at ~450 °C. Its orthorhombic framework structure (space group $C222_1$, 6.309(3) × 10.986(4) × 6.162(4) Å) contains one-dimensional helical pores ~6 Å in diameter along $\vec{c}$ (6 atoms/turn) that bind relatively well-ordered sodium countercations at 50% occupancy. The structure can also be described in terms of interlinked puckered double layers normal to $\vec{b}$ and parallel to the channels. Gallium is disordered over both tetrahedral framework sites, the gallium-richer and more negative site having closer sodium neighbors. The potassium compound cannot be made. Among analogous phases reported by others, $NaInSn_2$ has a lower symmetry and ordered cations, while $NaGaSn_5$ cannot be reproduced.

Introduction

As a guide in the search for new materials, it often can be helpful to seek models for structure and composition from related fields. In solid-state chemistry, one of the most intensively studied areas is the three-dimensional aluminosilicate framework structures built of vertex sharing $[SiO_{4/2}]^0$ and $[AlO_{4/2}]^{1-}$ tetrahedra, including the zeolites.[1] As aluminum cations are incorporated into these frameworks via condensation reactions, it is necessary to include an equal number of countercations, e.g., alkali-metal or tetraalkylammonium cations, into the structure to maintain charge balance. It is often the condensation and crystallization around a variety of countercation templates that result in the isolation of so many diverse open framework structures.[2,3]

In the system of valence compounds of main-group elements that are described by Zintl−Klemm formalisms,[4] the ability exists, in principle, to control the coordination geometry about each atom by controlling its formal oxidation state.[5] Thus a gallium monoanion, Ga^{1-}, is isoelectronic with the neutral group-14 metal Sn^0, and both atoms therefore have a very strong, even dominant, preference for tetrahedral bonding. With these building blocks it should be possible to build main-group-element framework structures from interbonded gallium and tin atom tetrahedra that are either analogues of aluminosilicates (without oxygen) or afford new tetrahedral framework structures. (Good space-filling in a crystalline array is of course another requirement.) To date at least two types of Zintl phases have been isolated that are in fact isostructural with microporous oxide framework structures. These are the clathrate-I valence compounds with the general formula $A_{8-x}T_{46-y}$ (A = Na−Cs, Ba; T = group 13, 14, 15 element mixtures), in which the framework T positions are those of Al and Si in sodalite,[6] and the clathrate-II type compounds Cs_7Si_{136} and Na_xSi_{136} ($3 < x < 11$),[7] wherein the framework is isotypic with the tetrahedral centers in the aluminosilicate ZSM-39.[3] In the present study, an examination of the tin-rich regions of the ternary system Na−Ga−Sn has resulted in the synthesis, isolation, and structural determination of the new Zintl phase $NaGaSn_2$. This has a novel all-metal tetrahedral framework of gallium and tin with large one-dimensional channels that is without precedent among oxides. Although all-tetrahedral Zintl phase structures are known, including the isoelectronic gray tin (diamond type) and NaTl, NaIn, and LiGa (stuffed diamond), nearly all have relatively compact structures.[8]

Experimental Section

Syntheses. The general techniques were as previously described.[9] All materials were handled in a N_2-filled glovebox that had a moisture level below 0.1 ppm (volume). An initial sample of composition "$NaGa_{0.9}Sn_2$" was prepared on a 500-mg scale by weighing stoichiometric amounts of the elements sodium (Alfa, 99.9+%), tin (Johnson-Matthey, 99.999%), and gallium (Johnson-Matthey, 99.99%) into a tantalum tube on which one end had been previously welded. The tantalum tube was crimped shut and welded and then placed inside a silica jacket that was evacuated and sealed. This was heated to 800 °C over a 1-day period, held there for 3 days, and then slowly cooled to room temperature over a 10-day period. Powder X-ray analysis of this sample showed it to be a mixture of 10% NaSn and 90% of a phase subsequently established to be $NaGaSn_2$. A single-phase sample of the compound (to Guinier powder diffraction) was subsequently synthesized by mixing stoichiometric amounts of the component elements and repeating the above procedure but with a slower heating ramp to 800 °C, holding for 1 day, and cooling to room temperature over a 4-day period.

[⊗] Abstract published in *Advance ACS Abstracts,* November 15, 1996.

(1) Newsam, J. M. In *Solid State Chemistry−Compounds*; Cheetham, A. K., Day, P., Eds.; Oxford University Press: Oxford, UK, 1993; Chapter 7.

(2) Occelli, M. L.; Robson, H. E., Eds. *Synthesis of Microporous Materials: Molecular Sieves* Eds.; van Nostrand Reinhold: New York, 1992; Vol. 1.

(3) Mejer, W. M.; Olson, D. H. *Atlas of Zeolitic Structure Types*, 2nd ed.; Butterworth Publ.: London, 1987.

(4) (a) Zintl, E. *Angew. Chem.* **1939**, *52*, 1. (b) Klemm, W.; Busmann, E. *Z. Anorg. Allg. Chem.* **1963**, *319*, 297.

(5) Schäfer, H. *Annu. Rev. Mater. Chem.* **1985**, *15*, 1.

(6) (a) Gallmeier, J.; Schafer, H.; Weiss, A. *Z. Naturforsch.* **1969**, *24B*, 665. (b) Westerhaus, W.; Schuster, H. U. *Z. Naturforsch.* **1977**, *32B*, 1365. (c) Menke, H.; von Schnering, H.-G. *Z. Anorg. Allg. Chem.* **1973**, *395*, 223. (d) von Schnering, H.-G.; Menke, H. *Z. Anorg. Allg. Chem.* **1976**, *424*, 108. (e) Nesper, R.; Curda, J.; von Schnering, H.-G. *Angew. Chem.* **1986**, *98*, 369. (f) von Schnering, H.-G. *Nova Acta Leopoldina* **1985**, *59*, 168. (g) Zhao, J.-T.; Corbett, J. D. *Inorg. Chem.* **1994**, *33*, 5721. (h) Kuhl, B.; Czybulka, A.; Schuster, H.-U. *Z. Anorg. Allg. Chem.* **1995**, *621*, 1.

(7) Cros, C.; Pouchard, M.; Hagenmuller, P. *J. Solid State Chem.* **1970**, *2*, 570.

(8) Parthé, E. In *Modern Perspectives in Inorganic Crystal Chemistry*, Parthé, E., Ed.; Kluwer Academic Publishers, Dordrecht, Holland, 1992; p 177.

(9) Zhao, J.-T.; Corbett, J. D. *Inorg. Chem.* **1995**, *34*, 378.

S0002-7863(96)01975-0 CCC: $12.00

Table 1. Lattice Constants of the $NaGaSn_2$ Component Observed in Products from a Variety of Starting Compositions

loaded composition	*a* (Å)	*b* (Å)	*c* (Å)	*V* (Å^3)
$NaGa_{0.90}Sn_2$ (16)[a]	6.309(3)	10.986(4)	6.162(4)	427.1(7)
$NaGaSn_3$ (23)	6.294(4)	10.983(4)	6.169(4)	426.4(2)
$NaGaSn_{1.9}$ (20)	6.309(7)	11.017(8)	6.142(7)	427(1)
$NaGaSn_2$ (18)	6.316(3)	10.985(9)	6.154(3)	427.0(9)
$NaGaSn_2$ (21)	6.309(5)	11.009(7)	6.142(5)	427(1)
$NaGaSn_2$ (21)	6.307(7)	11.009(7)	6.149(3)	427(1)
$NaGaSn_5$ (17)[b]	6.315(6)	11.029(5)	6.127(7)	427(1)
$NaGaSn_2$ (CAD4)	6.315(2)	10.984(3)	6.161(2)	427.4(2)
$NaGaSn_3$ (20)	6.311(10)	10.989(9)	6.149(9)	427(1)

[a] The number of indexed lines that were refined is given in parentheses. [b] Trigonal indexing of the Guinier pattern gave a = 6.338(8) Å and c = 6.157(11) Å.

The first product had a silvery appearance and was brittle. Several crystals were isolated and sealed into thin-walled capillary tubes. Once the structure had been established, the orthorhombic lattice constants were refined from 16 indexed lines from the powder pattern with a nonlinear least-squares method and NIST silicon as an internal standard to be a = 6.309(3) Å, b = 10.986(4) Å, c = 6.162(4) Å, V = 427.1(7) Å^3. The calculated powder pattern for this phase agreed in detail very well with that observed for the second sample synthesized, which places impurity phase levels at less than 3−5% in equivalent scattering power.

Analysis of Guinier powder X-ray diffraction data for other compositions indicated that tin-richer samples, e.g. $NaGaSn_3$, always resulted in mixtures of $NaGaSn_2$ and elemental tin, while gallium-rich compositions yielded $NaGaSn_2$ and an unidentified phase of approximate composition $Na_2Ga_2Sn_3$. A perhaps-equivalent phase $Na_2In_2Sn_3$ has been reported in the Na−In−Sn phase diagram, although no information is available about its exact stoichiometry or structure.[10] The lack of an appreciable phase width in $NaGaSn_2$ is supported by the relatively invariant lattice constants and unit cell volumes refined from patterns of a number of preparations listed in Table 1. The only samples among these that appeared single phase by X-ray Guinier powder diffraction methods were those loaded with the composition $NaGaSn_2$.

Structural Determination. Laue photographs were used to determine which crystal was most suitable for structural determination. Diffraction data were collected at room temperature on an Enraf-Nonius CAD4 diffractometer using Mo Kα radiation. Cell constants and orientation matrices for data collection were determined from a least-squares refinement of the setting angles of 25 centered reflections. In total, 1645 reflections were measured for the primitive orthorhombic cell in four (h,±k,±l) octants up to 2θ = 50°; of these 838 reflections were observed ($I/\sigma(I) > 3$). No violations of a *C*-centering condition were observed, and additional absences uniquely indicated the correct space group is $C222_1$ (No. 20). With an absorption correction based on the average of three ψ scans (μ = 177 cm^{-1}), the data reduced to 1012 independent observations (R_{ave} = 2.9%) of which 519 were observed ($I/\sigma(I)>3$). The structure was solved by direct methods with the aid of the program package TEXSAN.[11] Anomalous dispersion and secondary extinction were taken into account during the refinement. At a later point in the refinement, DIFABS was used to provide an improved absorption correction of the isotropically refined structure, as recommended by the authors of the program.[12]

During the above refinement, it became evident that the gallium and tin atoms were mixed over the two framework sites, and so their sum was constrained to unity at each site. We did not fix the stoichiometric proportions of the atoms or the relative amounts on each site, although to avoid serious coupling of the occupancies with the scale factor, one site was held constant while the other site was refined. This was iterated until the refinement converged at the reported compositions. In addition, the initial sodium position (4*a*) on a 2-fold axis was observed to have an unusually large and anisotropic temperature factor (B = 17(2), U_{22}/U_{11} = 14.4). Much more reasonable anisotropic temperature factors (B_{iso} = 7(1) Å^2, U_{22}/U_{11} = 1.6) and distances resulted when this atom was refined as a split position at half occupancy.

Table 2. Selected Data from the Single-Crystal Refinement of $NaGaSn_2$

empirical formula	$NaGaSn_2$
fw	382.99
crystal system	orthorhombic
space group, *Z*	$C222_1$ (No. 20), 2
lattice constants[a]	
a (Å)	6.309(3)
b (Å)	10.986(4)
c (Å)	6.162(2)
V (Å^3)	427.1(7)
density (calcd), g/cm^3	5.110
μ(Mo Kα), cm^{-1}	177.04
rel transm coeff range	0.886−1.141
R/R_w (%)[b]	3.3/4.3

[a] Guinier powder data with Si as an internal standard, λ = 1.540562 Å, 22 °C. [b] $R = \sum||F_o| - |F_c||/\sum|F_o|$; $R_w = [\sum w(|F_o| - |F_c|)^2/\sum w(F_o)^2]^{1/2}$; $w = 1/\sigma_F^2$.

The final refined composition was $NaGa_{0.97(5)}Sn_{2.03(5)}$ with fully occupied network sites as the only constraint. The anisotropic refinement of all atoms resulted in R(F), R_w values of 3.3, 4.3% at convergence. The maximum and minimum peaks in the final difference Fourier map were 1.23 e$^-$/Å^3 (1.7 Å from Na1) and −1.07 e$^-$/Å^3. A check of the other enatiomer gave higher R, R_w factors, 3.4, 4.5%; thus the orientation reported is the correct one.

Some data collections and refinement data are given in Table 2, the atom positions and isotropic-equivalent ellipsoid values are listed in Table 3, and the bond distances appear in Table 4. Additional crystallographic data and the anisotropic displacement parameters are given in the Supporting Information. These and the F_o/F_c data are also available from J.D.C.

Results and Discussion

The compound $NaGaSn_2$ represents a new structure type both in Zintl chemistry and as a rare helical-pore framework type.[3] The first isolated and one of the most often studied examples is zeolite β, which crystallizes in the presence of a chiral template as an intergrowth of the two possible orientations.[13] A more recent nonsilicate example is $NaZnPO_4{\cdot}H_2O$ reported by Harrison et al. with a complex helical pore framework and both sodium cations and water within the channels.[14]

The structure of $NaGaSn_2$, shown in Figure 1 in a view down the *c*-axis, is built of helical chains of six atoms per turn that are composed of a disordered mixture of tetrahedrally-bound gallium and tin in an overall 1:2 ratio. Distortions within the framework lead to interbond angles from 105.0° to 124.7°. The four-bonded atoms, the refined composition $NaGa_{0.97(5)}Sn_{2.03(5)}$, and the single phase synthesis at the composition $NaGaSn_2$ are all consistent with a Zintl formulation. The helical chains run parallel to the *c*-axis and enclose the sodium cations. Two vertices about each network atom are associated with one channel while the other two bonds connect it to two adjacent helices. An alternative view is a layered structure that is cross-linked along the long *b*-axis. Figure 2 is a view of a single layer along $\vec{b}$ with the Sn2/Ga2 atoms darker, while Figure 3 is a [100] view of the interlinked layers. (The same layers are also evident in the orthogonal view in Figure 1.) In this description, the layers are composed of tetrahedrally bonded atoms with all Sn2/Ga2 atoms four-bonded within the layer while the Sn1/Ga1 sites on the surfaces of each layer are three-bonded within the layer and form a fourth bond to an Sn1/Ga1

(10) Blase, W.; Cordier, G.; Kniep, R.; Schmidt, R. *Z. Naturforsch.* **1989**, *44b*, 505.
(11) TEXSAN, version 6.0, Molecular Structure Corp.; The Woodlands, TX, 1990.
(12) Walker, N.; Stuart, D. *Acta Crystallogr.* **1983**, *A39*, 158.
(13) (a) Treacy, M. M.; Newsam, J. M. *Nature (London)* **1988**, *332*, 249. (b) Newsam, J.; Treacy, M.; Koetsier, W.; DeGruyter, C. B. *Proc. R. Soc. London A* **1988**, *420*, 375.
(14) Harrison, W. T. A.; Gier, T.; Stucky, G.; Broach, R.; Bedard, R. *Chem. Mater.* **1996**, *8*, 145.

Table 3. Refined Atomic Positions, Thermal Parameters, and Occupancies for $NaGaSn_2$

atom	Wykoff posn.	*x*	*y*	*z*	B_{eq}[a]	occup.: Sn(σ)/Ga, %
Sn1/Ga1	8*c*	0.3506(1)	0.37949(8)	0.0802(1)	1.59(4)	75(3)/25
Sn2/Ga2	4*b*	0	0.2627(1)	1/4	1.75(6)	54(2)/46
Na[b]	8*c*	0.359(2)	-0.046(2)	−0.068(2)	7(1)	

[a] $B_{eq} = (8\pi^2/3)\sum_i\sum_j U_{ij} a_i^* a_j^* \vec{a}_i \vec{a}_j$. [b] 50% occupancy.

Table 4. Selected Distances (Å) and Angles (deg) in $NaGaSn_2$

M1−M1[a]	2.826(2)	Na−M1	3.13(1)	Na−Na	3.69(4)
M1−M1	2.817(2)	Na−M1	3.34(1)	Na−Na	2.87(4)
M1−M2	2.763(1)	Na−M1	3.38(2)	Na−Na	1.31(4)[b]
M1−M2	2.733(2)	Na−M1	3.43(2)		
M2−M1	2.763(2) ×2	Na−M1	3.52(1)		
M2−M1	2.733(2) ×2	Na−M1	3.60(2) ×2		
$\bar{d}$	2.7664	Na−M2	3.01(1)		
		Na−M2	3.43(2)		
		Na−M2	3.47(2)		
M1−M1−M1	105.06(3)	M1−M2−M1	124.66(7)		
M1−M1−M2	124.58(3)	M1−M2−M1	105.74(3) ×2		
M1−M1−M2	105.97(6)	M1−M2−M1	105.05(4) ×2		
M1−M1−M2	104.74(5)	M1−M2−M1	110.28(8)		
M1−M1−M2	108.81(5)				
M2−M1−M2	107.02(4)				

[a] M1 = 0.75(3) Sn, 0.25 Ga; M2 = 0.54(2) Sn, 0.46 Ga. [b] Split position.

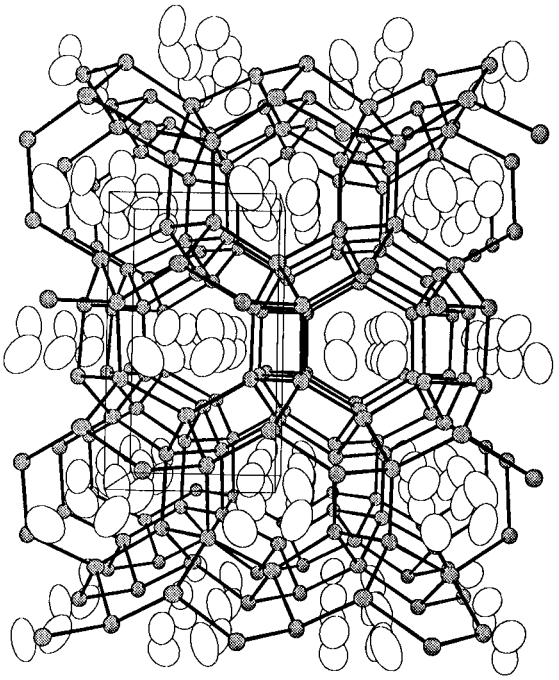

Figure 1. The structure of $NaGaSn_2$ looking down the *c*-axis ($\vec{b}$ vertical) with the Ga/Sn atoms gray. The ellipsoids are shown at 75% probability.

atom on the adjoining layer either above or below. This construction gives rise to both the channels along the *c*-axis seen in Figure 1 and a network of five membered rings interconnecting the layers along $\vec{a}$. Two of the latter are highlighted in black in Figure 3.

The nominally tetrahedral Sn−Ga network appears to be the most important feature in determining this structure, and this leaves the sodium atoms in less than ideal positions, as is often the case. Both regular displacements from the apparent channel center and a 50:50 splitting of the sodium sites are involved in the multiple sites represented in Figure 1. First, the channels are spiral, not cylindrical, with a six-atom repeat, and so regular (hypothetical) sodium sites at $z = 0, 1/2$ are regularly displaced along $\vec{a}$ from the projected channel center (left and right). This undisplaced arrangement is shown in a side [010] view in Figure 4a with the sodium atoms drawn as open spheres. Actually, atoms refined in these sites presented very large ellipsoids elongated along [$0\bar{2}\bar{1}$] more or less normal to this view, but a relatively small (1.3 Å) 50:50 split of the site with more sensible distances refined readily. The basis for this distortion is found in the poor environment of the central Na position shown in Figure 4a, which lies on a 2-fold axis at (0.359,0,0). Such a position centers a very flattened tetrahedron (wide gray lines; the two smallest angles are 52°) with Na−(Sn,Ga) distances (twice each) of 3.15 (to M2) and 3.19 Å (M1), while the next four neighbors more-or-less normal to this figure are 3.42 and 3.49 Å (narrow lines, all to M1). Displacements or disorder are common in such environments, and the driving force here appears to be not the gain of more network neighbors, which stay at eight (<3.60 Å), but closer and more sodium contacts, particularly with the gallium-richer M2 site which should carry more of the negative charge and be smaller. (The smaller Na−Sn distances in other compounds are in the neighborhood of 3.18−3.35 Å,[15] while those for Na−Ga are typically 2.93(1)−3.10 Å.[16]) Thus the distortion leads from two Na−M2 separations at 3.15 Å to one each at 3.01, 3.43, and 3.47 Å, while one Na−M1 contact in this range is lost with no change in the average distance. The five Na−M1 distances average 3.36 Å (omitting two more at 3.60 Å) while the three Na−M2 average a smaller 3.30 Å. The converse is even more distinctive; the more negative M2 atom has six 50% sodium neighbors (two each at 3.01, 3.43, and 3.47 Å) while M2 has only five (3.13, 3.34, 3.38, 3.43, and 3.52 Å).

Attempts to substitute larger cations such as potassium in the $NaGaSn_2$ structure resulted in the formation of only ca. K_2Ga_3 and $K_8Ga_8Sn_{38}$,[17] a compound with the cubic clathrate-I structure and a framework isotypic with Rb_8Sn_{44}[6g] and the zeolite sodalite (without oxygen). In the latter structure, all of the main-group elements also exhibit tetrahedral coordination,

(15) (a) Müller, W.; Volk, K. *Z. Naturforsh.* **1977**, *32B*, 709. (b) Müller, W.; Volk, K. *Z. Naturforsh.* **1978**, *33B*, 275.

(16) (a) Ling, R. G.; Belin, C. *Acta Crystallogr.* **1982**, 38B, 1101. (b) Frank-Cordier, U.; Cordier, G.; Schäfer, H. *Z. Naturforsch.* **1982**, *37b*, 119. (c) Charbonnel, M.; Belin, C. *J. Solid State Chem.* **1987**, *67*, 210.

(17) von Schnering, H.-G., private communication, 1994. Kröner, R. Doctoral Dissertation, University of Stuttgart, 1989.

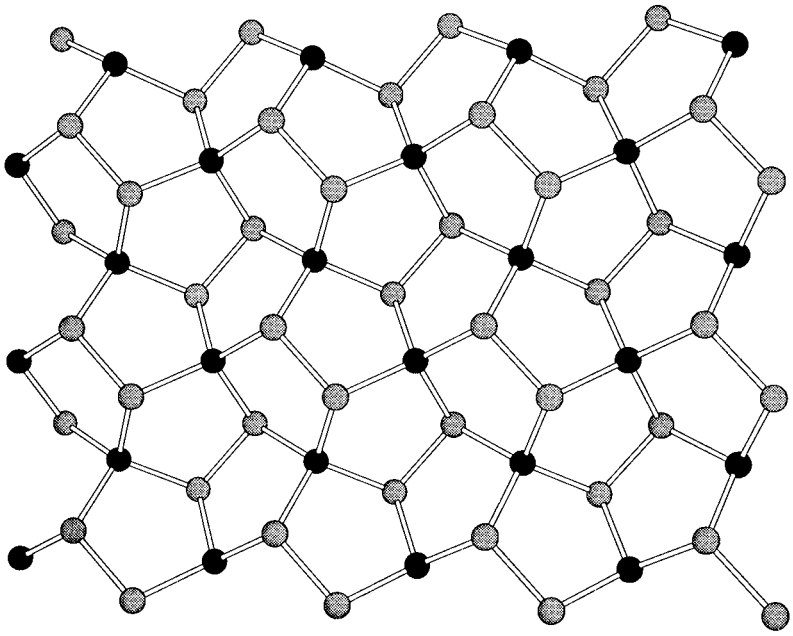

Figure 2. A view of a single layer in the structure of $NaGaSn_2$ looking down the *b*-axis at the *a*−*c* plane. The four-bonded black spheres represent Sn2/Ga2 atoms, while the three-bonded gray spheres are Sn1/Ga1 atoms. ($\vec{a}$ is horizontal.)

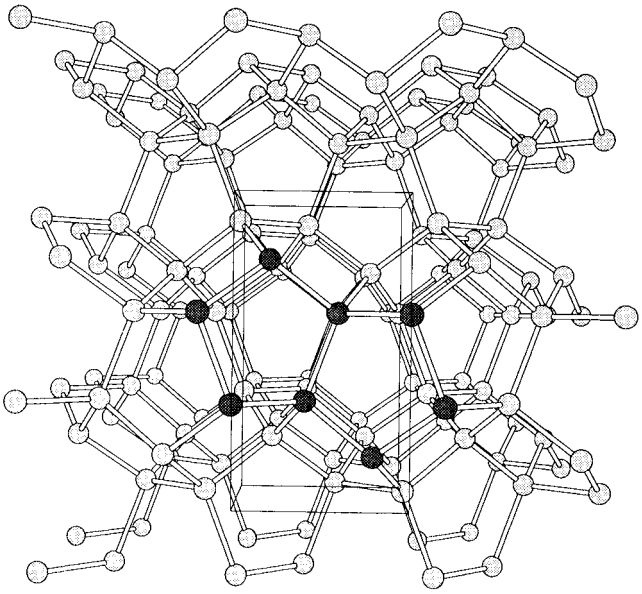

Figure 3. A view of the $NaGaSn_2$ structure down the *a*-axis that highlights the horizontal double layers in the structure, which are centered by Sn2/Ga2 and interconnected along $\vec{b}$ (vertical) by Sn1/Ga1 bonds. (The same layers in an orthogonal view lie horizontal in Figure 1.) Two of the five-membered rings formed by the cross linking of layers are emphasized. These rings form the edges of the channels and are seen more clearly in Figure 1.

but the connections between the rings are different than in $NaGaSn_2$, resulting in smaller channels along all three axes instead of a large channel along only one. The alkali-metal preferences between the two structural types appear to be a function of not only the cation proportions but also the size of the channel and, in turn, the size of the alkali-metal. In the clathrate structure, each hexagonal ring is stacked on others with 45° rotations as each subsequent layer is added. Since the pore diameter in each framework is slightly different (clathrate 5.24 and 6.02 Å; $NaGaSn_2$ 6.01−6.12 Å between surface atom centers), the unusual inverse alkali-metal preferences may be attributable in part to the cation proportions and these distances. In the $NaGaSn_2$ structure, the sodium cations down the channels are alternately displaced from the channel center in $\vec{a}$ so as to be 3.01−3.52 Å from the framework walls (Figure 4b). This makes the shortest (center to center) Na−Na distance 3.69(4) Å (outside of the false distances created by the split position). For such reasons, potassium cations are evidently unstable in the present network structure as their larger size would force them toward the center of the channel and into even shorter contacts with the framework walls and, especially, with other intrachannel cations. The complete story must, of course, also include the unique stability of the competing phases, especially the more suitable environment for potassium in the clathrate. The clathrate structure is additionally favored by the lower cation proportion, about 50% of that of $NaGaSn_2$.

A structure closely related to that of $NaGaSn_2$ has been described for $NaInSn_2$ by Blase et al.[12] Although similar in appearance, the indium analogue has a primitive orthorhombic cell in space group $P2_12_12_1$. A close examination of the framework positions in $NaInSn_2$ reveals it to be a slightly distorted and less symmetric form of the $NaGaSn_2$ framework, with positional differences of up to 20 σ. The F_o data for $NaInSn_2$ clearly confirm the lack of *C*-centering, although it is close to that point (the translation is [0.482,0.489,0.031] instead of [$^1/_2$,$^1/_2$,0]) when the unit cell axes are placed in the same orientation as for $NaGaSn_2$). A major difference between the structures is the cation position within the channel. Substitution of indium for gallium gives a roughly 0.3-Å increase in the pore diameter which favors the movement of the cation further from the center of the channel (in projection) and closer to one side in order to maintain proper bonding distances to the framework. Both of these differences can be seen in Figure 5, a projection down the $\vec{b}$-axis of $NaInSn_2$. Comparison with the *c*-axis view of $NaGaSn_2$ in Figure 1 shows a clear distortion of the network in $NaInSn_2$ and different positions for the (unsplit) cations within the channels. Similar observations have been made in other systems, in $CsNa[La_9I_{16}N_4]$ where changes in either the cation or framework result in a shift of the cation positions within a structurally unchanged channel,[18] or in the recent report on the microporous catalyst HSAPO-34[19] in which two separate channel coordination sites were identified for

(18) Lulei, M. F.; Corbett, J. D. *Eur. J. Solid State Inorg. Chem.* **1996**, *33*, 241.

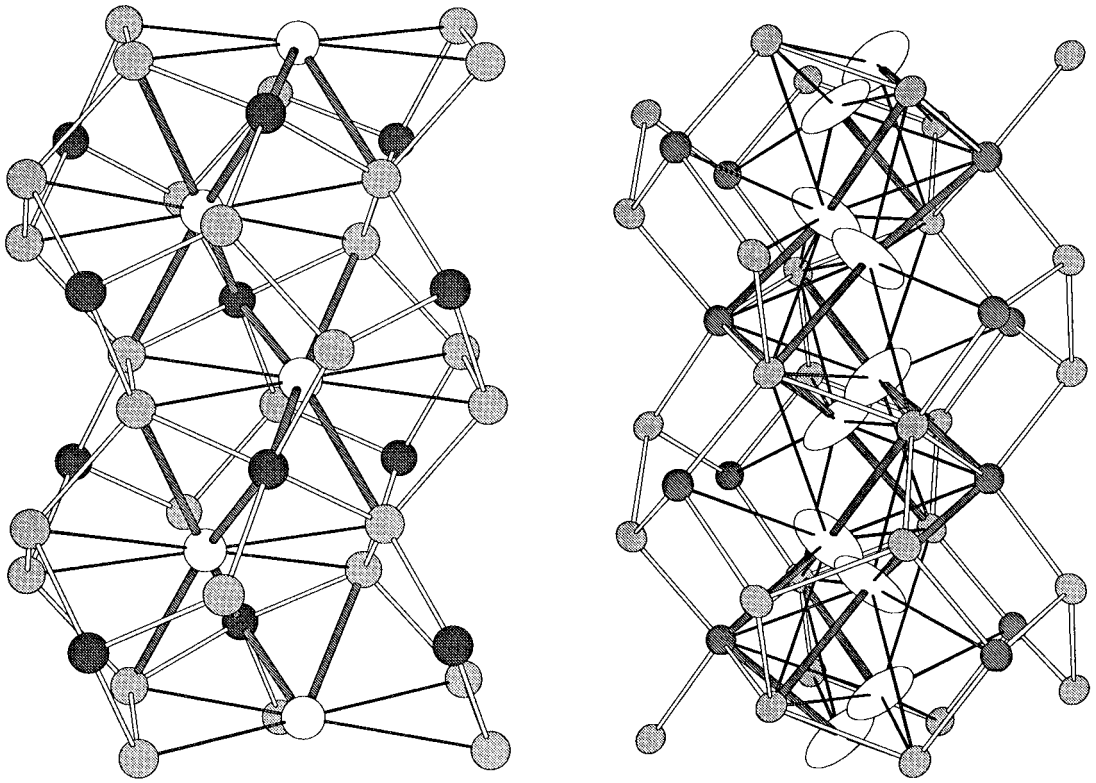

Figure 4. (a) A nearly [010] view of the position and coordination of the (hypothetical) central sodium positions (open circles) within the channels in $NaGaSn_2$ (arbitrary spheres, $\bar{c}$ vertical). Note the zig-zag nature of the sodium sites as these follow the spiral walls; the same cations appear left and right in the channels in Figure 1. Some basis for the formation of split sodium positions is shown by their environment; the wide gray Na−(Sn,Ga) connections mark the four shorter distances (3.15−3.19 Å), and the narrow solid lines, the four larger separations (3.42−3.49 Å). (b) Orthogonal [100] view of the refined sodium positions in $NaGaSn_2$. The wider lines between the (50%) sodium cations and the framework represent separations of 3.01−3.13 Å, while the solid lines mark those in the 3.34−3.52-Å range. The darker spheres are the more negative, gallium-richer M2 sites. (The sodium ellipsoids are shown at 75% probability).

hydrogen-bound water and hydronium ions. In the case of the two $NaTrSn_2$ microporous Zintl phases (Tr = Ga, In), the sodium cation adopts a position nearer to the center of the channel in $NaGaSn_2$ where it can maximize its framework coordination (judging from bond distances), while in $NaInSn_2$, the cation bonding is optimized (again, judging by distances) when the cation is closer to one framework wall.

Another Zintl compound in the Na−Ga−Sn system has also been reported, $NaGaSn_5$.[20] This was synthesized from a melt of the same composition (without note of yield), and its structure was refined in the trigonal space group $P3_112$ ($R = 0.097$) with completely disordered p elements. However, the framework of the structure reported for $NaGaSn_5$ appears to be substantially the same as given here for *c*-centered orthorhombic $NaGaSn_2$, not only in appearance but also in metric details of both the cell ($b_{orth} = \sim 3^{1/2} b_{trig}$) and the atom positions, given that the framework sites are intermixed on conversion between the trigonal and orthorhombic descriptions. (The above article contains an erroneous illustration of the reported $NaGaSn_5$ structure.) Otherwise, the reported tin-richer structure evidently differs mainly in the accommodation of half as many cations in the helical pores; the calculated powder patterns are distinguishable. However, our attempts to synthesize a $NaGaSn_5$ phase have led only to mixtures of $NaGaSn_2$ and considerable tin metal, as shown in Table 1.

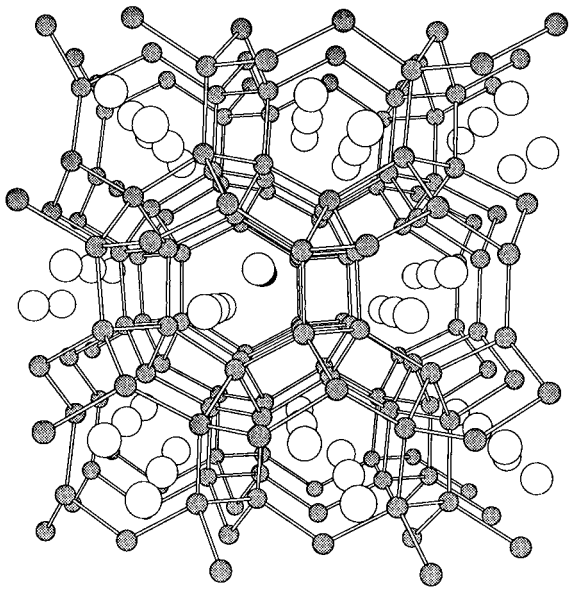

Figure 5. The structure of $NaInSn_2$ viewed down the *b*-axis.[12] The sodium sites are the open spheres.

Conclusions

We have successfully synthesized and characterized a new non-oxide framework structure composed of tetrahedrally-bound gallium and tin. The framework contains one-dimensional pores

(19) Smith, L.; Cheetham, A. K.; Morris, R. E.; Marchese, L.; Thomas, J. M.; Wright, P. A.; Chen, J. *Science* **1996**, *271*, 799.
(20) Blase, W.; Cordier, G. *Z. Naturforsch.* **1988**, *43b*, 1017.

approximately 6 Å in diameter that hold the sodium countercations. This compound illustrates the versatility of Zintl−Klemm formalisms not only to help understand but also to control a structure via the electron count and characteristic bonding of the constituent main-group elements.

Acknowledgment. The authors would like to thank Leonard Thomas for maintaining the single-crystal X-ray diffraction equipment. This research was supported by the Office of the Basic Energy Sciences, Materials Science Division, Department of Energy. The Ames Laboratory is operated for the DOE by Iowa State University under Contract No. W-7405-Eng-82.

Supporting Information Available: Tables of extended data collection and refinement information and anisotropic displacement parameters (2 pages). See any current masthead page for ordering and Internet access instructions.

JA961975F